Chemical Orthogonality Between Antibiotics and Quorum Sensing Receptor Ligands: Computational Screening of Natural Products Using Machine Learning

Maxwel Adriano Abegg *

Posted Date: 21 April 2026

doi: 10.20944/preprints202604.1392.v1

Keywords: quorum sensing; machine learning; natural products; antibiotics; pharmacophore; chemical orthogonality; COCONUT; drug discovery

 doi:10.20944/preprints202604.1392.v1

Article

Chemical Orthogonality Between Antibiotics and Quorum Sensing Receptor Ligands: Computational Screening of Natural Products Using Machine Learning

Maxwel Adriano Abegg

Federal University of Amazonas (UFAM), Institute of Exact Sciences and Technology (ICET), Graduate Program in Sciences, Technology and Health (PPGCTS), Itacoatiara, Amazonas, Brazil; maxabegg@gmail.com or maxwel.abegg@ufam.edu.br

Abstract

Sub-inhibitory (sub-MIC) antibiotics modulate bacterial quorum-sensing (QS) networks, but whether this modulation involves direct receptor engagement or indirect stress-mediated mechanisms remains unresolved. To address this, we trained a Random Forest classifier (ECFP4; scaffold-split AUC = 0.958; Y-randomization separation = 0.482) on 3,324 ChEMBL-curated compounds to predict engagement with LuxR-family N-acyl-homoserine lactone (AHL) receptors across six bacterial species. Clinical antibiotics (n = 54) scored near zero (mean P(QS) = 0.014), including those with documented sub-MIC QS effects ($p = 0.36$ vs. undocumented), suggesting that sub-MIC modulation operates via transcriptional reprogramming rather than direct binding. Large-scale screening of 36,132 antibacterial compounds (Broad Institute) confirmed a negative correlation between P(QS) and antibacterial activity (Spearman $\rho = -0.086$; $p < 10^{-60}$), robust across species-stratified and MW-stratified analyses. Screening of 731,587 natural products (NPs) from the COCONUT database identified 41 non-AHL candidates with P(QS) > 0.3 within the applicability domain, including the confirmed QS inhibitor Honaucin A and the marine antibiotics Korormicins. Independent pharmacophore analysis against a 10-AHL reference panel confirmed greater similarity of NP candidates to AHLs relative to antibiotics (Gobbi-Tanimoto: 0.108 vs. 0.037; Mann-Whitney $p = 0.006$). The results demonstrate quantitative chemical orthogonality between antibacterials and QS modulators and identify NPs as priority hypotheses for experimental validation of dual function — QS modulation at sub-MIC and antibacterial activity at elevated concentrations.

Keywords: quorum sensing; machine learning; natural products; antibiotics; pharmacophore; chemical orthogonality; COCONUT; drug discovery

1. Introduction

The ecological role of antibiotics in microbial communities has been reassessed over the past two decades. The classical view of antibiotics as chemical weapons has been challenged by observations that their environmental concentrations are typically below the minimum inhibitory concentration (MIC), suggesting alternative biological functions under ecologically relevant conditions [1,2]. Goh et al. [3] first demonstrated that sub-MIC concentrations modulate the expression of hundreds of bacterial genes, and Linares et al. [4] and Yim, Wang and Davies [5] formalized this observation as the hypothesis that antibiotics function primarily as signaling molecules, with growth inhibition being a concentration-dependent emergent property.

Subsequent studies confirmed sub-MIC QS modulation by several clinically important antibiotics, including azithromycin, tobramycin, ciprofloxacin and cefoperazone [6–9]. A central mechanistic question remains, however: does this modulation involve direct engagement of receptor

 doi:10.20944/preprints202604.1392.v1

binding sites — implying structural mimicry of autoinducers — or does it occur indirectly, via stress-mediated transcriptional reprogramming? The distinction has implications for anti-virulence drug design [10,11]: if antibiotic scaffolds can engage QS receptors, they can serve as starting points; if not, anti-virulence strategies require exploration of distinct chemical space.

Chemoinformatic analyses indicate that QS autoinducers occupy a compact chemical space distinct from that of antibiotics [12,13], and machine-learning models have been applied to QS modulators [14]. However, no study has systematically scored the clinical antibiotic arsenal using models trained on QS receptor-engagement data. In this work, a validated Random Forest classifier for AHL-type LuxR receptors is employed to: (i) test the hypothesis of direct engagement across clinical antibiotics (n = 54); (ii) evaluate large-scale orthogonality across the Broad Institute antibacterial library (n = 36,132); and (iii) screen 731,587 natural products (NPs) from the COCONUT database for dual-function candidates.

2. Materials and Methods

2.1. Training Data and Model Architecture

QS receptor engagement data for LuxR-family AHL receptors were curated from ChEMBL for eight receptors across six bacterial species: LasR, RhlR and PhzR (Pseudomonas aeruginosa PAO1), CviR (Chromobacterium violaceum), TraR (Agrobacterium tumefaciens), LuxR (Aliivibrio fischeri and Vibrio harveyi), and SdiA (Escherichia coli K12). The multi-species approach captures pan-AHL pharmacophore features conserved within the LuxR family rather than species-specific binding determinants. After curation (removal of duplicates, salt forms and potential data-leakage compounds such as ciprofloxacin and tamoxifen), the primary model comprised 153 actives (activity threshold ≤ 10 μM in IC50, EC50, Ki or Kd) and 3,171 inactives spanning 1,976 Bemis-Murcko scaffolds. ECFP4 fingerprints (Morgan radius 2, 2,048 bits; RDKit v2024.03) were computed. A Random Forest classifier (500 trees, class-balanced weights; scikit-learn v1.3) was evaluated under 5-fold scaffold-split cross-validation (AUC-ROC = 0.958 ± 0.047; AUC-PR = 0.847 ± 0.108; MCC = 0.751 ± 0.072).

2.2. Validation and Sensitivity Analysis

Y-randomization with 100 label-permutation iterations confirmed non-spurious learning (random AUC = 0.496 ± 0.025; separation = 0.482). External validation employed 61 compounds across five main categories (AHL agonists, antagonists, antibiotics with documented QS effects, antibiotics without documented QS effects, and negative controls), including the alkylquinolones PQS and HHQ from the pqs system. The applicability domain (AD) was defined by the Tanimoto distance to the nearest neighbor in the training set (NN threshold ≥ 0.33). As a sensitivity analysis, a permissive model (≤ 50 μM, 889 actives, 4,015 total, scaffold-split AUC = 0.931 ± 0.018) was trained in parallel; all conclusions were compared across both models (Supplementary Table S2).

2.3. Antibacterial Datasets and Natural Product Screening

Two antibacterial datasets were scored: (1) 36,132 compounds from the Broad Institute screening library, classified as active (n = 24,521) or inactive (n = 11,611) by MIC thresholds across six species, scored with the 50 μM model; (2) 54 approved clinical antibiotics, annotated by pharmacological class, biosynthetic origin (natural product — NP, semi-synthetic — SS, fully synthetic — FS), primary target, spectrum, and documented sub-MIC QS effects. As an auxiliary exploratory analysis, scores were cross-referenced with intracellular permeability data in P. aeruginosa PAO1 from Leus et al. [15]; results, consistent with the main conclusion, are reported in the supplementary material deposited at Zenodo (10.5281/zenodo.19622234). The COCONUT library [16] (April 2026 dump) provided 731,587 valid NPs after SMILES validation and molecular-weight filtering (100–1,500 Da). Candidates were defined as NPs with P(QS) > 0.3 within the AD; the 0.3 threshold corresponds to the

 doi:10.20944/preprints202604.1392.v1

empirical inflection point at which the native-AHL to novel-candidate ratio transitions from noise-dominated to signal-dominated. Compounds of the "Fatty acyl homoserine lactones" class (native AHLs cataloged in COCONUT) were excluded a posteriori to identify genuinely non-AHL candidates.

2.4. Pharmacophore and Statistical Analysis

Pharmacophore similarity between NP candidates, reference AHLs and control antibiotics (ciprofloxacin, tetracycline, chloramphenicol, gentamicin, meropenem) was computed with Gobbi pharmacophore fingerprints (RDKit), using the mean Tanimoto coefficient against the AHL panel. Initial computations used a 5-AHL panel (3-oxo-C12-HSL, C4-HSL, 3-oxo-C6-HSL, C8-HSL, 3OH-C4-HSL); the panel was subsequently expanded to 10 AHLs (C4, C6, C8, C10, C12, C14 and 3-oxo-C6/-C8/-C10/-C12) to strengthen the validation. AHL-like pharmacophore presence (amides, lactones, homoserine lactone core) was quantified by SMARTS substructure search. Random Forest feature importances were extracted from scikit-learn's feature_importances_ attribute. Non-parametric tests (Mann-Whitney U, Kruskal-Wallis H with Bonferroni correction, Spearman correlation, partial Spearman controlling for MW + logP + TPSA) were performed in Python 3.12 with SciPy 1.12.

3. Results and Discussion

3.1. Model Performance and Specificity

The primary model (10 μM) achieved scaffold-split AUC = 0.958 ± 0.047, OOB AUC = 0.978 and Y-randomization separation = 0.482 (Figure 1A). In external validation, all 12 AHL agonists scored P(QS) > 0.83 (Figure 1B). Notably, PQS (0.911) and HHQ (0.828) — alkylquinolones of the pqs system, structurally distinct from AHLs — were also detected, suggesting partial pharmacophore overlap between AHL and quinolone signaling scaffolds despite belonging to different receptor families. AHL-like antagonists were recovered (furanone C-30: 0.957), while structurally divergent antagonists were not (mBTL: 0.029; savirin: 0.003), confirming specificity for AHL-type features. RF feature-importance analysis revealed signal concentration in a restricted subset of ECFP4 bits (bit 935 accounted for 2.1× the importance of the second most relevant), a pattern consistent with focused learning on the amide + lactone pharmacophores evidenced below (Figure 5; Supplementary Table S4). The UMAP chemical-space map (Figure 1C) shows that QS-active training compounds and clinical antibiotics occupy distinct regions, a direct visualization of the orthogonality quantified in the following sections.

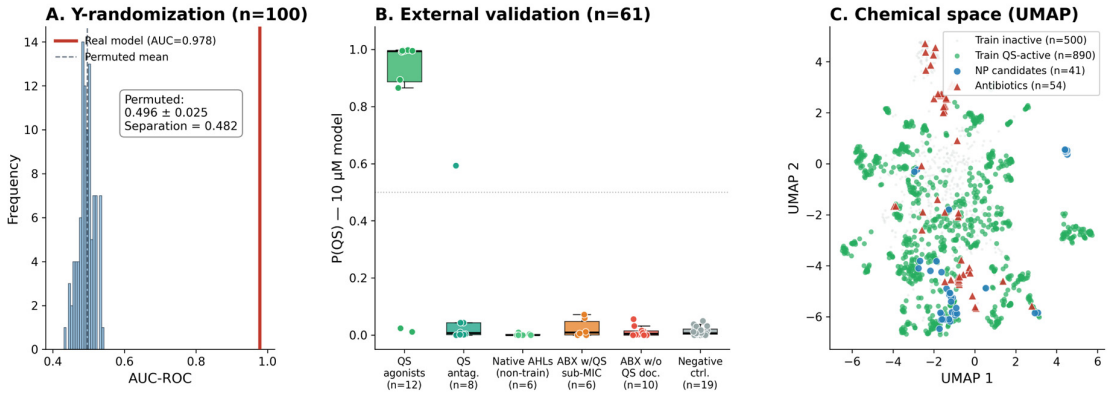

Figure 1. ***Model validation.*** (A) Y-randomization: AUC distribution across 100 label-permuted models (mean = 0.496 ± 0.025) versus real AUC (0.978); separation = 0.482. (B) External validation (n = 61): AHL agonists (n = 12), antagonists (n = 8), antibiotics with documented QS effects (n = 6), without QS documentation (n = 10) and negative controls (n = 19); the alkylquinolones PQS (0.911) and HHQ (0.828) were also evaluated. (C) UMAP of

 doi:10.20944/preprints202604.1392.v1

ECFP4 chemical space: QS-active training compounds (green) and antibiotics (triangles) occupy distinct regions; NP candidates (blue circles) interpose between clusters.

3.2. Chemical Orthogonality of Clinical Antibiotics

The 54 clinical antibiotics showed systematically low P(QS). Fluoroquinolones scored lowest (mean 0.000), followed by carbapenems (0.007), cephalosporins (0.009), penicillins (0.007), tetracyclines (0.003), aminoglycosides (0.012), and macrolides (0.068) (Kruskal-Wallis H = 28.10; p = 0.0005; Figure 2A). Stratification by biosynthetic origin revealed that natural products retained greater compatibility with QS receptors (NP = 0.021; SS = 0.014; FS = 0.008; KW p = 0.003; Figure 2B). In the AD-restricted analysis (n = 43), the global effect remained significant (p = 0.002), although the NP > SS pairwise comparison lost significance in the strict model (p = 0.19), suggesting contribution of marginal-potency compounds (10–50 μM) or limited statistical power. The seven antibiotics with documented sub-MIC QS modulation scored indistinguishably from the remaining 47 (mean 0.019 vs. 0.013; p = 0.36). This null result is mechanistically informative: if sub-MIC modulation involved direct receptor engagement, these antibiotics would score significantly higher, providing computational evidence in favor of indirect stress-mediated mechanisms.

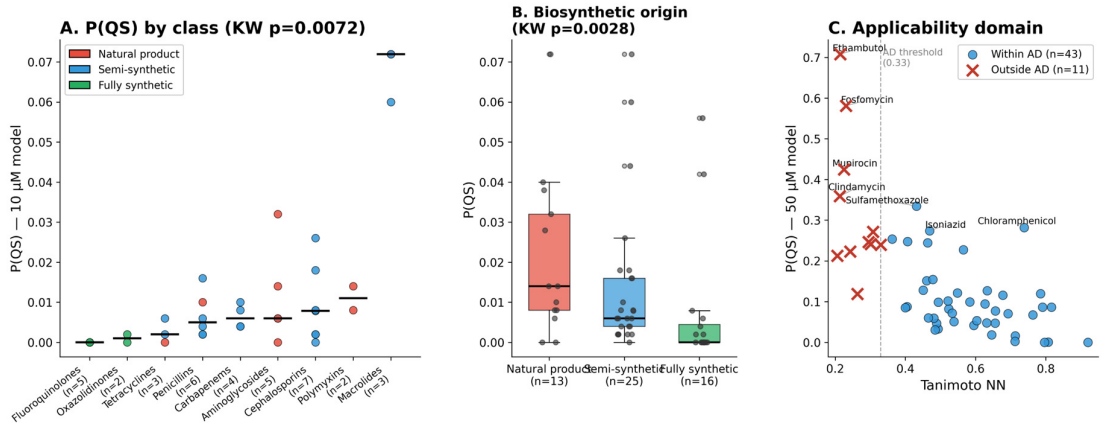

Figure 2. ***Curated antibiotics (n = 54; 10 μM model).*** (A) P(QS) by pharmacological class; parentheses indicate number of compounds per class. (B) Stratification by biosynthetic origin: NP = natural product (n = 13), SS = semi-synthetic (n = 25), FS = fully synthetic (n = 16); Kruskal-Wallis p = 0.003. (C) Applicability domain (50 μM model): compounds within AD (blue, n = 43) and outside AD (× red, n = 11), with labels for major false positives (ethambutol, fosfomycin, mupirocin).

3.3. Large-Scale Screening and Natural Product Library

Screening of 36,132 Broad Institute compounds (50 μM model) confirmed that active antibacterial compounds have systematically lower P(QS) than inactive ones (median 0.0003 vs. 0.0007; Mann-Whitney $p < 10^{-60}$; Figure 3A), a pattern that persisted across all molecular-weight bins from 100 to 800 Da (Figure 3B). The global Spearman correlation between P(QS) and antibacterial activity was negative and highly significant ($\rho = -0.086$; $p < 10^{-60}$; n = 36,132), with small magnitude — consistent with chemical orthogonality rather than strong biological antagonism. Species-stratified analysis yielded robust negative correlations for all organisms tested with adequate n: *E. coli* ($\rho = -0.23$; $p \approx 10^{-132}$; n = 11,078), *P. aeruginosa* ($\rho = -0.19$; $p \approx 10^{-137}$; n = 17,586), *S. pneumoniae* ($\rho = -0.11$; n = 4,699) and *M. tuberculosis* ($\rho = -0.08$; n = 11,718) — a biologically coherent pattern given that AHLs are predominantly Gram-negative signals. Among compounds with P(QS) ≥ 0.5, only 49.2% were antibacterially active, compared to 67.9% in the general population (inactive enrichment ratio = 1.58×). A minority fraction (~4%) combines high P(QS) and antibacterial activity, concentrating in chemically overlapping classes (long polyprenoids, acylhydrazones) that may represent genuine dual-function candidates — an interpretation consistent with the hypothesis rather than antagonistic to it.

 doi:10.20944/preprints202604.1392.v1

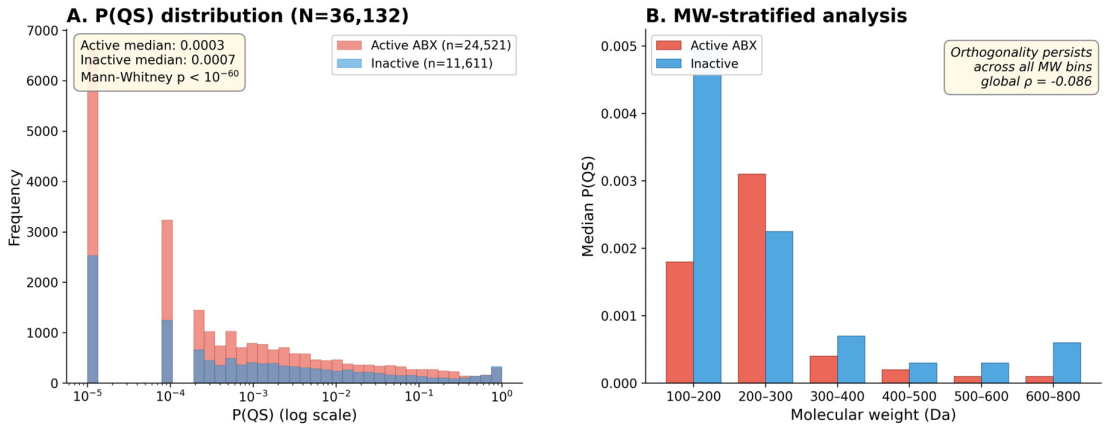

Figure 3. ***Large-scale screening of 36,132 antibacterial compounds (Broad Institute).*** (A) P(QS) distribution (50 μM model) for active antibacterials (n = 24,521) vs. inactives (n = 11,611); active median = 0.0003, inactive median = 0.0007 (Mann-Whitney $p < 10^{-60}$). (B) Median P(QS) stratified by molecular-weight bin: orthogonality persists across all bins 100–800 Da, refuting the MW confounder.

From the COCONUT library (731,587 valid NPs), 231,360 (31.6%) fell within the model AD — a substantially greater fraction than observed for the Broad library (~6.7%), indicating that NPs are structurally closer to the QS-modulator chemical space, even without necessarily scoring higher on average. Among within-AD NPs, 79 scored P(QS) > 0.3; of these, 38 were identified as native AHLs cataloged in COCONUT, whose detection by the model is expected and trivial. The remaining 41 candidates are structurally non-AHL NPs with pharmacophores compatible with LuxR-family receptors.

3.4. Non-AHL Candidates: Chemical Profile and Literature Evidence

A systematic literature search revealed that several of the 41 non-AHL candidates possess previously documented biological activity (Table 1). Three Korormicin compounds (G, J and K; P(QS) = 0.31–0.34) have experimentally confirmed antibacterial activity against *Vibrio cholerae* and *P. aeruginosa* PAO1 (MIC ~ 20 μM) via Na^+-NQR inhibition and reactive oxygen species production [17,18]. Honaucin A (P(QS) = 0.636) is a confirmed QS inhibitor isolated from the cyanobacterium *Leptolyngbya crossbyana*, which inhibits QS-dependent bioluminescence in *V. harveyi* BB120 [19]; its identification by the model without inclusion in training constitutes independent external validation. Thiolactone B4 (P(QS) = 0.556) is a thiolactonic analog structurally related to the autoinducing peptides of the Agr system in *S. aureus* [20]. Erdosteine (P(QS) = 0.585), a semi-synthetic mucolytic with anti-biofilm properties, carries thiolactone + amide [21]. Cepaciamide A (P(QS) = 0.371), isolated from *Burkholderia cepacia*, simultaneously carries amide and lactone. Fourteen of the 41 candidates simultaneously display both AHL central pharmacophores (amide and cyclic lactone).

Table 1. *Priority non-AHL NP candidates identified by COCONUT screening.*

Compound	P(QS)	Pharm. sim.	NP class	Antibacterial evidence	QS / pharmacophore evidence	Ref.
Honaucin A	0.636	0.155	Cyanolactone	n.r.	Confirmed QSI (V. harveyi); AHL analog	[19]
Erdosteine	0.585	0.127	Thiolactone	ATB potentiator; anti-biofilm	Thiolactone + amide	[21]

 doi:10.20944/preprints202604.1392.v1

Compound	P(QS)	Pharm. sim.	NP class	Antibacterial evidence	QS / pharmacophore evidence	Ref.
Thiolactone B4	0.556	0.377	N-acyl amine	Analogs modulate S. aureus	AIP analog (Agr system)	[20]
Caprolactin A	0.432	0.180	Piperid. alkaloid	Antibacterial class (MIC ~5 μg/mL)	Amide + lactam	[22]
Caprolactin B	0.420	0.180	Piperid. alkaloid	Same as A	Amide + lactam	—
Triacetylfusigen	0.412	0.051	Siderophore	Fungal siderophore	Amide + lactone	—
Biemamide B	0.372	0.132	Lipopeptide	Marine ATB class	5 amides; signal-like features	—
Cepaciamide A	0.371	0.094	Piperid. alkaloid	ATB-producing organism	QS+ org. (CepI/R); amide + lactone	[23]
Cladospamide A	0.368	0.115	Amide	n.r.	Amide + lactone	—
Bacillamidin C	0.344	0.202	Piperid. alkaloid	ATB-producing genus	3 amides; peptidic scaffold	—
Korormicin G	0.336	0.142	Polyketide	Confirmed ATB (P. aeruginosa MIC ~20 μM)	Amide + lactone; Na^+-NQR	[17]
Biemamide D	0.326	0.130	N-acyl amine	Same as Biemamide B	5 amides	—
Korormicin J	0.308	0.223	Polyketide	Confirmed ATB (Vibrio spp.)	Amide + lactone	[18]
Korormicin K	0.308	0.216	Polyketide	Confirmed ATB (Vibrio spp.)	Amide + lactone	[18]

n.r. = not reported; QSI = quorum-sensing inhibitor; ATB = antibiotic; Piperid. = piperidinic.

3.5. Independent Pharmacophore Validation

Pharmacophore analysis with Gobbi fingerprints, recalculated against an expanded 10-AHL reference panel (C4–C14, 3-oxo and 3-hydroxy), confirmed that NP candidates are significantly more similar to AHLs than are control antibiotics (median Tanimoto pharmacophore similarity: NP = 0.108 vs. ABX = 0.037; Mann-Whitney $p = 0.006$; Figure 4A). The 2D Morgan similarity showed a concordant result (NP = 0.327 vs. ABX = 0.106; $p = 0.004$). The correlation between P(QS) and pharmacophore similarity strengthened with the expanded panel (Spearman $\rho = 0.464$; $p = 3.2 \times 10^{-4}$; Figure 4B; versus $\rho = 0.357$ with 5 AHLs), demonstrating that the model captures real pharmacophore features detectable by entirely independent metrics. Substructure analysis revealed that NP candidates carry on average 2.15 amides and 0.80 cyclic lactones per molecule, compared with 0.80 and 0 for control antibiotics. Approximately 15% of candidates (6/41) carry the intact homoserine lactone core (SMARTS NC1CCOC1=O), while none of the control antibiotics do (Figure 5A). Fourteen of the 41 candidates simultaneously carry amide and cyclic lactone — the two central pharmacophores of AHL binding to LuxR receptors (Figure 5B).

 doi:10.20944/preprints202604.1392.v1

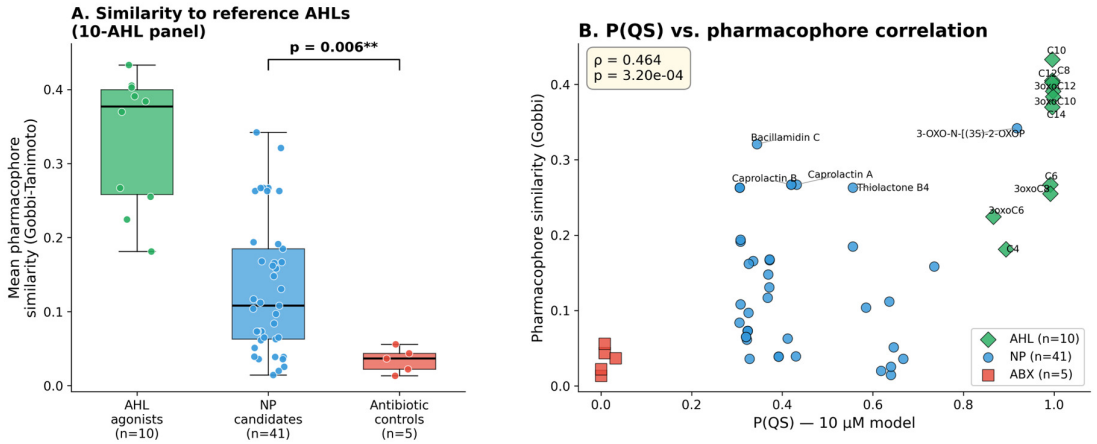

Figure 4. ***Independent pharmacophore validation.*** (A) Gobbi-Tanimoto similarity to reference AHLs by group: AHL agonists (n = 10), NP candidates (n = 41), and control antibiotics (n = 5); Mann-Whitney NP vs. ABX p = 0.006. (B) Correlation between P(QS) (10 μM model) and Gobbi pharmacophore similarity, computed against the expanded 10-AHL panel: Spearman ϱ = 0.464 ($p = 3.2 \times 10^{-4}$); diamonds = AHL, circles = NP, squares = ABX.

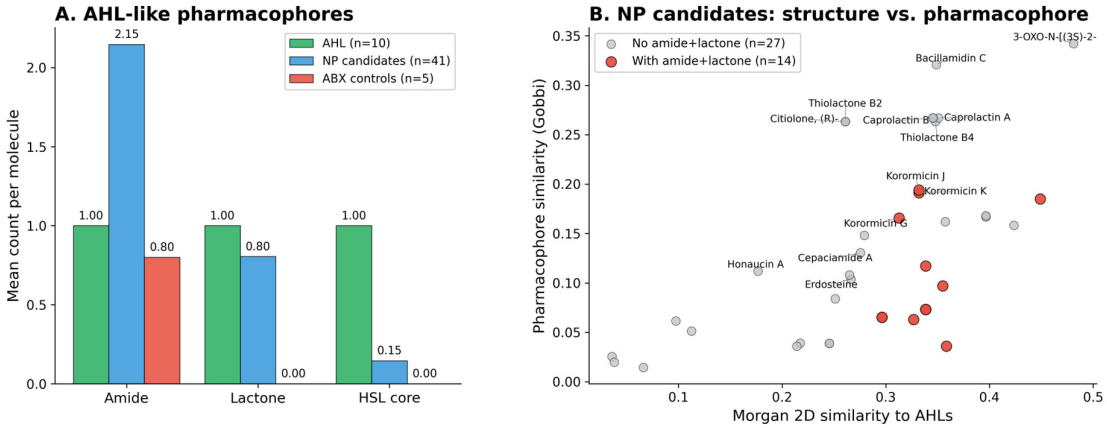

Figure 5. ***AHL-like structural features in candidates.*** (A) Mean count of AHL-like pharmacophores (amide, cyclic lactone, homoserine lactone core) per molecule in reference AHLs (n = 10), NP candidates (n = 41), and control antibiotics (n = 5). NP candidates carry 2.15 amides/molecule vs. 0.80 in ABX, and 6/41 (14.6%) carry the intact HSL core. (B) NP candidates plotted by 2D Morgan vs. Gobbi similarity: NPs with amide + cyclic lactone (n = 14) highlighted in red; annotations on key compounds identified in the literature search.

3.6. Sensitivity Analysis

The permissive model (≤ 50 μM, 889 actives) reproduced the central findings: orthogonality (mean P(QS) = 0.149 for antibiotics), null result for QS-documented (p = 0.67), biosynthetic-origin effect (KW p = 0.003; NP > SS Bonferroni p = 0.0006). False positives were identified (ethambutol: 0.708; fosfomycin: 0.581), but were outside the AD and eliminated by the strict model (ethambutol: 0.042; fosfomycin: 0.040; isoniazid: 0.274 → 0.000). Supplementary Table S2 systematically compares findings across both models.

3.7. Mechanistic Synthesis and Implications

The results support a tripartite framework of antibiotic–QS interaction. In Mode 1 (direct engagement), dedicated QS modulators bind LuxR receptors and score P(QS) > 0.7. In Mode 2 (indirect perturbation), clinical antibiotics modulate QS at sub-MIC via stress-mediated transcriptional reprogramming — not receptor binding — evidenced by equivalent scoring of QS-

 doi:10.20944/preprints202604.1392.v1

documented and undocumented antibiotics and by the placement of 93.3% of antibacterial compounds outside the AD. In Mode 3 (potential dual function), NPs with elevated P(QS) and AHL-like pharmacophores may represent compounds with genuine receptor-engagement potential at sub-MIC and antibacterial activity at elevated concentrations, exemplified by the Korormicins (MIC ~ 20 μM against *P. aeruginosa*; amide + lactone). The fraction of NPs within the AD (31.6%) — substantially greater than synthetics (~6.7%) — is consistent with the hypothesis that NPs retain ancestral signaling features lost during synthetic optimization for antibacterial potency. For anti-virulence drug discovery, the observed orthogonality implies that repurposing conventional antibiotics as direct QS modulators is improbable, and that the anti-virulence pipeline is correctly exploring novel chemical territory. The NP candidates identified here may represent, given the in silico data, concrete starting points, and it appears reasonable to recommend for the five priority candidates (Korormicin G, Honaucin A, Thiolactone B4, Cepaciamide A, Erdosteine): direct binding assays (SPR, ITC) with recombinant LuxR receptors; QS-reporter assays at sub-MIC; and dose-response curves to separate therapeutic windows of dual function.

3.8. Limitations

The model specifically captures AHL-like pharmacophore features; structurally divergent antagonists are not detected, and systems such as PqsR/MvfR, AgrC/AIP and AI-2/LsrB were not explicitly modeled due to limited availability of large-scale screening data. The 10 μM threshold, although more clinically relevant than 50 μM, remains above the typical EC50 of natural autoinducers (~ nM). The interpretation of orthogonality partially depends on the assumption that Random Forest does not extrapolate well outside the AD — comparison with other architectures (XGBoost, gradient boosting, deep neural networks) and formal uncertainty quantification via conformal prediction remain as relevant future directions. The pharmacophore validation, orthogonal to ML, does not substitute for experimental validation; all analyses in this work are computational, and the candidates identified are hypotheses, not validated compounds. Code, full data, and supplementary figures are deposited in a public repository (Zenodo DOI: 10.5281/zenodo.19622234).

4. Conclusions

This work demonstrates, quantitatively and through three independent lines of evidence (validated ML model, large-scale screening of 36,132 compounds, pharmacophore analysis), chemical orthogonality between antibacterial compounds and AHL-type QS receptor ligands. Clinical antibiotics — including those with documented sub-MIC QS modulation — score P(QS) near zero, suggesting that the sub-MIC effects reported in the literature operate predominantly via indirect stress-mediated mechanisms, not direct receptor engagement. The orthogonality is robust to activity threshold variation (10 vs. 50 μM), persists in species- and MW-stratified analyses, and is not a permeability artifact.

Screening of 731,587 natural products from the COCONUT bank identified 41 non-AHL candidates with pharmacophores compatible with LuxR receptors, validated by independent pharmacophore analysis and by literature evidence of antibacterial activity (Korormicins) and QS inhibition (Honaucin A) obtained without inclusion of these compounds in training. These candidates — predominantly polyketides, piperidinic alkaloids, and marine lipopeptides — constitute priority hypotheses for experimental validation of dual function, with apparent potential for anti-virulence assays via QS modulation at sub-MIC and classical antibacterial activity (bactericidal/bacteriostatic) at higher concentrations. The results presented here are computational and generate testable hypotheses, not mechanistic claims about individual compounds; experimental confirmation in direct binding assays and QS-reporter systems remains the essential next step.

 doi:10.20944/preprints202604.1392.v1

5. AI Use Declaration

This work used the Claude Opus 4.7 model (Anthropic) as an assistive tool in: support for manuscript writing and formatting; implementation and debugging of Python scripts for data processing, cheminformatic computations (RDKit, scikit-learn, UMAP), and figure generation; bibliographic look-up; and preparation of the supplementary material. All scientific and methodological decisions — study conception, target selection, manual curation of training datasets (ChEMBL), algorithm choice, results interpretation, and final manuscript approval — were the author's exclusive responsibility, with systematic verification of AI-assisted outputs against raw data and primary literature. No step involved AI-generated or fabricated data; all computation was executed locally in a Python/conda environment controlled by the author.

Supplementary Materials:

Data Availability Statement: All code, intermediate data, supplementary tables and high-resolution figures are publicly available at Zenodo under the Creative Commons Attribution 4.0 International (CC BY 4.0) license: https://doi.org/10.5281/zenodo.19622234.

Conflicts of Interest: The author declares no conflict of interest.

References

1. Davies, J.; Spiegelman, G. B.; Yim, G. The world of subinhibitory antibiotic concentrations. *Curr. Opin. Microbiol.* **2006**, *9*, 445–453.
2. Romero, D.; Traxler, M. F.; López, D.; Kolter, R. Antibiotics as signal molecules. *Chem. Rev.* **2011**, *111*, 5492–5505.
3. Goh, E. B.; Yim, G.; Tsui, W.; McClure, J.; Surette, M. G.; Davies, J. Transcriptional modulation of bacterial gene expression by subinhibitory concentrations of antibiotics. *Proc. Natl. Acad. Sci. USA* **2002**, *99*, 17025–17030.
4. Linares, J. F.; Gustafsson, I.; Baquero, F.; Martínez, J. L. Antibiotics as intermicrobial signaling agents instead of weapons. *Proc. Natl. Acad. Sci. USA* **2006**, *103*, 19484–19489.
5. Yim, G.; Wang, H. H.; Davies, J. Antibiotics as signalling molecules. *Philos. Trans. R. Soc. B* **2007**, *362*, 1195–1200.
6. Tateda, K.; Comte, R.; Pechere, J. C.; Köhler, T.; Yamaguchi, K.; Van Delden, C. Azithromycin inhibits quorum sensing in Pseudomonas aeruginosa. *Antimicrob. Agents Chemother.* **2001**, *45*, 1930–1933.
7. Skindersoe, M. E.; Alhede, M.; Phipps, R.; Yang, L.; Jensen, P. O.; Rasmussen, T. B.; et al. Effects of antibiotics on quorum sensing in Pseudomonas aeruginosa. *Antimicrob. Agents Chemother.* **2008**, *52*, 3648–3663.
8. Carvalho, R. D.; et al. Aminoglycosides and quorum-sensing regulation in Vibrio cholerae. *Microbiol. Res.* **2021**, *253*, 126876.
9. El-Far, A.; et al. Cephalosporin derivatives inhibit violacein production. *J. Mol. Struct.* **2023**, *1292*, 136134.
10. Grandclément, C.; Tannières, M.; Moréra, S.; Dessaux, Y.; Faure, D. Quorum quenching: role in nature and applied developments. *FEMS Microbiol. Rev.* **2016**, *40*, 86–116.
11. Whiteley, M.; Diggle, S. P.; Greenberg, E. P. Progress in and promise of bacterial quorum sensing research. *Nature* **2017**, *551*, 313–320.
12. O'Shea, R.; Moser, H. E. Physicochemical properties of antibacterial compounds. *J. Med. Chem.* **2008**, *51*, 2871–2878.
13. Jonkergouw, C.; et al. Exploration of chemical diversity in intercellular quorum sensing signalling systems. *Angew. Chem. Int. Ed.* **2024**, *63*, e202314469.
14. Mahmoud, A. S.; et al. Machine learning approaches for prediction of quorum sensing modulators. *Comput. Biol. Med.* **2025**, *186*, 109612.
15. Leus, I. V.; Weeks, J. W.; Bonifay, V.; Smith, L.; Richardson, S.; Zgurskaya, H. I. Property space mapping of Pseudomonas aeruginosa permeability to small molecules. *Sci. Rep.* **2022**, *12*, 8220.

 doi:10.20944/preprints202604.1392.v1

16. Soares, A. C.; et al. COCONUT 2.0: an integrative natural product database. *Nucleic Acids Res.* **2024**, *52*, D1302–D1310.
17. Barker, N. L.; et al. Antibiotic Korormicin A kills bacteria by producing reactive oxygen species. *J. Bacteriol.* **2019**, *201*, e00718-18.
18. Tebben, J.; Motti, C.; Hay, M. E.; Tapiolas, D. M.; Steinberg, P. D. Five new korormicins from Pseudoalteromonas sp. J010. *Mar. Drugs* **2014**, *12*, 2802–2815.
19. Choi, H.; Mascuch, S. J.; Villa, F. A.; Byrum, T.; Teasdale, M. E.; Smith, J. E.; et al. Honaucins A–C, potent inhibitors of inflammation and bacterial quorum sensing. *Chem. Biol.* **2012**, *19*, 589–598.
20. Mayville, P.; Ji, G.; Beavis, R.; Yang, H.; Goger, M.; Novick, R. P.; Muir, T. W. Structure-activity analysis of synthetic autoinducing thiolactone peptides from Staphylococcus aureus. *Proc. Natl. Acad. Sci. USA* **1999**, *96*, 1218–1223.
21. Cazzola, M.; Page, C. P.; Matera, M. G. Erdosteine: possible roles in management of biofilms. *Pulm. Pharmacol. Ther.* **2018**, *53*, 62–70.
22. Zhang, H.; et al. Isolation and structure of caprolactins and related piperidine alkaloids from marine bacteria. *J. Nat. Prod.* **2021**.
23. Huber, B.; Riedel, K.; Hentzer, M.; Heydorn, A.; Gotschlich, A.; Givskov, M.; et al. The cep quorum-sensing system of Burkholderia cepacia. *Microbiology* **2004**.